Accepted Manuscript

Oral supplementation with cocoa extract reduces UVB-induced wrinkles in hairless mouse *skin*

Jong-Eun Kim, Dasom Song, Junil Kim, Jina Choi, Jong Rhan Kim, Hyun-Sun Yoon, Jung-Soo Bae, Mira Han, Sein Lee, Ji Sun Hong, Dayoung Song, Seong-Jin Kim, Myoung-Jin Son, Sang-Woon Choi, Jin Ho Chung, Tae-Aug Kim, Ki Won Lee

PII: S0022-202X(16)00457-7

DOI: 10.1016/j.jid.2015.11.032

Reference: JID 171

To appear in: *The Journal of Investigative Dermatology*

Received Date: 15 July 2015

Revised Date: 26 November 2015

Accepted Date: 30 November 2015

Please cite this article as: Kim J-E, Song D, Kim J, Choi J, Kim JR, Yoon H-S, Bae J-S, Han M, Lee S, Hong JS, Song D, Kim S-J, Son M-J, Choi S-W, Chung JH, Kim T-A, Lee KW, Oral supplementation with cocoa extract reduces UVB-induced wrinkles in hairless mouse *skin*, *The Journal of Investigative Dermatology* (2016), doi: 10.1016/j.jid.2015.11.032.

Oral supplementation with cocoa extract reduces UVB-induced wrinkles in hairless mouse *skin*

Jong-Eun Kim[1, 2, †], Dasom Song[1, 2, †], Junil Kim[3,†], Jina Choi[3,4], Jong Rhan Kim[1,2], Hyun-Sun Yoon[5,6,7], Jung-Soo Bae[5,6], Mira Han[5,6], Sein Lee[1, 2], Ji Sun Hong[1,2], Dayoung Song[3,4], Seong-Jin Kim[3], Myoung-Jin Son[8], Sang-Woon Choi[9], Jin Ho Chung[5,6,10], Tae-Aug Kim[3,4,*], and Ki Won Lee[1,2,10,*]

[1]WCU Biomodulation Major, Center for Food and Bioconvergence, Department of Agricultural Biotechnology, Seoul National University, Seoul, Republic of Korea; [2]Advanced Institutes of Convergence Technology, Seoul National University, Suwon, Republic of Korea; [3]CHA Cancer Institute and [4]Department of Biochemistry, School of Medicine, CHA University, Seongnam, Republic of Korea; [5]Department of Dermatology, Seoul National University College of Medicine, Seoul, Republic of Korea; [6]Institute of Human-Environment Interface Biology, Seoul National University, Seoul, Republic of Korea; [7]Department of Dermatology, Seoul National University Boramae Hospital, Seoul, Republic of Korea; [8]Health Foods Team, Lotte R&D Center, Seoul, Republic of Korea; [9]CHAUM Life Center, School of Medicine, CHA University, Seoul, Republic of Korea; [10]Institute on Aging, Seoul National University, Seoul, Republic of Korea

[†] These authors contributed equally to this work

[*]Correspondence to: Ki Won Lee, kiwon@snu.ac.kr, Department of Agricultural Biotechnology, Seoul National University, Seoul 151-921, Republic of Korea. Tel.: 82-2-880-4853. Fax: 82-2-873-5095.

Tae-Aug Kim, takim@cha.ac.kr, CHA Cancer Institute, Department of Biochemistry, School of Medicine, CHA University, Seongnam 463-400, Republic of Korea. Tel: +82-31-881-7177, Fax: +82-31-881-7185

Abstract

Cacao beans contain various bioactive phytochemicals that could modify the pathogeneses of certain diseases. Here, we report that oral administration of cacao powder (CP) attenuates UVB-induced skin wrinkling by the regulation of genes involved in dermal matrix production and maintenance. Transcriptome analysis revealed that 788 genes are down- or up-regulated in the CP supplemented group, compared to the UVB-irradiated mouse skin controls. Among the differentially-expressed genes, cathepsin G and serpin B6c play important roles in UVB-induced skin wrinkle formation. Gene regulatory network analysis also identified several candidate regulators responsible for the protective effects of CP supplementation against UVB-induced skin damage. CP also elicited anti-wrinkle effects via inhibition of UVB-induced MMP-1 expression in both the human skin equivalent model and human dermal fibroblasts (HDFs). Inhibition of UVB-induced AP-1 via CP supplementation is likely to affect the expression of MMP-1. CP supplementation also down-regulates the expression of cathepsin G in HDFs. 5-(3′,4′-dihydroxyphenyl)-γ-valerolactone, a major in vivo metabolite of CP, showed effects similar to CP supplementation. These results suggest that cacao extract may offer a protective effect against photoaging by inhibiting the breakdown of dermal matrix, which leads to an overall reduction in wrinkle formation.

Keywords: cacao; UVB; skin wrinkle; MMP-1; cathepsin G

Introduction

Many natural products are known to influence the development of skin structures and its biological functions. Cacao beans have the antioxidant capacity higher than the capacity provided by green teas and red wine (Lee *et al.*, 2003; Subhashini *et al.*, 2010). The antioxidant activity of cacao can modify the pathogeneses of a different spectrum of diseases, including the cardiovascular diseases, cancer, and other chronic conditions (Park *et al.*, 2014). Recent studies have demonstrated the beneficial effects of cacao consumption are associated with human health, especially with the improved condition of the skin (Park *et al.*, 2014; Scapagnini *et al.*, 2014). Cacao provides positive effects on the skin structure and the dermal microcirculation (Katz *et al.*, 2011; Neukam *et al.*, 2007), and its topical preparations are able to protect the skin from the oxidative damages arising from ultraviolet (UV) radiation (Katz *et al.*, 2011). Besides the photoprotection against UVB-induced erythema, long-term ingestion of cacao also ameliorates aberrant skin conditions by increasing the blood flow to the cutaneous and subcutaneous tissues to increase the skin density and hydration (Heinrich *et al.*, 2006). Our previous studies have shown that cacao inhibits skin cancer growth and skin inflammation both *in vitro* and *in vivo* (Kang *et al.*, 2008; Kim *et al.*, 2010; Lee *et al.*, 2006). Although there are accumulating evidences that cacao consumption can improve the skin health, the molecular mechanisms responsible for these beneficial effects have not been thoroughly investigated.

Skin wrinkling is a typical characteristic of photoaging that results from chronic exposure to solar UV radiation. Repeated exposure to UV light decreases procollagen production and breaks down collagen fibers. The process is partially due to the overexpression of matrix metalloproteinases (MMP) (Fisher *et al.*, 1997; Ichihashi *et al.*, 2009; Xu and Fisher, 2005). Our previous studies demonstrated that cathepsin G regulates MMP expression and UVB-induced skin photoaging (Son *et al.*, 2009; Son *et al.*, 2012). Cathepsins comprise a family of serine proteases whose members are classified into A, B, C, D, E, G, H, and L groups, according to their substrate specificities (Son *et al.*, 2009). Cathepsins B, D, K, and G may act as biomarkers in photoaged human skin (Zheng *et al.*, 2011). Cathepsin G is a single 30-kDa polypeptide released by the neutrophils and the UVA-irradiated normal human fibroblasts (Son *et al.*, 2009). Inhibitors of cathepsin G may be useful for the prevention of UVB-induced photoaging since they could ameliorate the ECM damage and MMP upregulation (Son *et al.*, 2012). Serpin b6 is a member of the superfamily of serine protease inhibitors known as serpins. Serpins bind with serine proteases involved in inflammatory processes, coagulation, fibrinolysis, tumorigenesis and apoptosis. The association of serpin b6 with cathepsin G has been postulated to inhibit cathepsin G activity (Scott *et al.*, 2007).

In this study, we first examined the protective effect of CP on UVB-induced wrinkle formation in hairless mice, then we showed gene expression profiles using RNA sequencing analysis in comparison with several other well-known food materials used to modify skin health (Cho *et al.*, 2007; Marini *et al.*, 2012). To better investigate the anti-photoaging effects of CP and the implications for clinical settings, we measured its effects using a human dermal fibroblasts (HDF) and human skin equivalent (HSE) model.

Results

Oral administration of CP reduces UVB-induced wrinkle formation and prevents UVB-induced collagen degradation

To investigate the effect of CP on wrinkle formation, the dorsal skins of hairless mice were exposed to UVB with low and high concentrations of CP (CL, 39.1 mg/kg, CH, 156.3 mg/kg) and pycnogenol (Pyc, 625 mg/kg) for 8 weeks as described (Fig. 1A). UVB-induced wrinkle formation was markedly reduced in the CP-administered groups (Fig. 1B). Quantification of skin wrinkle severity through the assessment of the area of wrinkling (Fig. 1C) and visual wrinkle grade (Fig. 1D) confirmed a significant decrease in wrinkle formation in the CP groups. We then stained the skin samples of the mice with Masson's trichrome staining to observe the effect of CP on amorphous collagens of the skin (Fig. 1E). Collagen levels gradually recovered in the CP groups to an extent greater than the UVB-irradiated group (Fig. 1E, Supplement figure 1). The physical aesthetics of the CP groups were similar or superior to those of the pycnogenol-treated group (Fig. 1 C, D and E). Taken together, these results suggest that oral administration of CP reduces UVB-induced wrinkle formation and prevents UVB-induced collagen degradation.

Expression profiling of differentially-expressed genes (DEGs) mediated by CP supplementation and/or UVB-irradiation of mouse skin tissue

To identify genes associated with the UVB-protective effect of CP supplementation in skin, we systematically analyzed the transcriptome from the mice exposed to UVB-irradiation and/or administrated with CP and pycnogenol. The heat map of differentially expressed genes (DEGs) in the UVB-irradiated mice indicated that 788 genes were up- or down-regulated by at least one concentration of CP supplementation (Fig. 1F). Among the 788 DEGs, 156 genes were up-regulated by UVB compared to control and down-regulated by CH compared to UVB-IR (Fig. 1G); and 199 genes were down-regulated by UVB-IR compared to the controls and up-regulated by CH compared to the UVB irradiated group (Fig. 1H). Supplementation with CH elicited transcriptomic recovery on the up- and down-regulated genes post-UVB-IR (Fig. 1G and 1H). Furthermore, CP administration shows more impact on transcriptomic recovery than the recovery induced by Pycnogenol (Fig. 1G and 1H), suggesting that CP may be a more potent anti-photoaging agent than Pycnogenol.

Expression patterns of genes associated with anti-photoaging

To further characterize gene expression patterns, we identified the genes associated with anti-photoaging effects using the related gene ontology (GO) terms including Extracellular Matrix Disassembly (Fig. 2A), Cell Adhesion (Fig. 2B), Lipid Metabolic Process (Fig. 2C), and Proteinaceous Extracellular Matrix (Fig. 2D and Supplementary Table 1). The gel-like extracellular matrix (ECM) is the largest component of the dermal skin layer and is comprised of a variety of fibrous structural proteins, including collagens, elastin, laminin, and proteoglycans such as dermatan sulfate and hyaluronan (Bradley *et al.*, 2015). Differentially expressed genes in ECM disassembly indicated that CP-fed mice had markedly inverted changes in their UVB-mediated transcriptomes (Fig. 2A). CP significantly diminished UVB-induced cathepsin G (Ctsg) expression. Interestingly, the effect of CP on these expression patterns was more significant than that of pycnogenol (Fig. 3A). Among the various serpin b6 genes, CP supplementation specifically enhanced the expression of serpin b6c (Fig. 3B). These findings suggest that both inhibition of cathepsin G and induction of serpin B6c by CP supplementation may contribute to a protective effect against UVB-induced wrinkle formation. To identify potential mediators of the changes in transcriptome expression patterns, we constructed a Gene Regulatory Network (GRN) analysis composed of the DEGs in Figure 3C, and significantly enriched transcription factors (TFs) obtained from the TF-target relationships derived from the Encyclopedia of DNA Element (ENCODE) Data (Consortium, 2012; Gerstein *et al.*, 2012) and SignaLink database (Fazekas *et al.*, 2013) (Fig. 3D and 3E). Thus**,** GRN analysis identifies the mediators involved in the anti-photoaging effects of CP.

CP prevents UVB-induced MMP-1 upregulation in HDF and in HSE layers

To better understand whether the anti-wrinkling effects of CP in mice could be relevant for clinical settings, we examined the effect of CP on collagenase (MMP-1) in HDF and HSE layers. CP treatment elicited a decrease in MMP-1 protein expression in a concentration-dependent manner and significantly suppressed the mRNA levels of UVB-induced MMP-1 (Fig. 4A and 4B). Furthermore, CP inhibited UVB-induced AP-1 transactivation (Fig. 4C). These inhibitory effects arose within a concentration range that did not significantly affect cell viability in the presence of UVB irradiation (Fig 4D). These results suggest that CP may downregulate both UVB-induced MMP-1 protein and gene expression through the suppression of UVB-induced AP-1 transcriptional activity in HDF. To confirm the effects of CP on cathepsin G expression, we measured the expression of cathepsin G in HDF. Cathepsin G expression is decreased by CP treatment in HDF (Fig. 4E). Next, to verify whether the anti-wrinkle effect of CP in mice and in vitro could be applied to humans, we examined the effect of CP on collagenase (MMP-1) in HSE as described in supplement Fig 2. Immunohistochemical staining showed that CP markedly inhibited UVB-induced MMP-1 levels with increasing levels of CP (Fig. 4F).

DHPV significantly decreased UVB-induced MMP-1 protein expression, gene transcription and AP-1 transactivation in HDF.

To investigate the metabolite effect of CP on UVB-induced wrinkle formation, 5-(3′,4′-dihydroxyphenyl)-γ-valerolactone (DHPV) (Fig. 5A), a major metabolite form of CP in the body, was used as shown in the previous study (Urpi-Sarda *et al.*, 2009). The effect of DHPV on UVB-induced MMP-1 protein and gene expression *in vitro* have been measured (Figure 5B and 5C). DHPV decreased MMP-1 protein expression (Fig. 5B) and significantly suppressed UVB-induced MMP-1 mRNA level (Fig. 5C), compared with those of the UVB-irradiated cells. We also examined the effect of DHPV on AP-1 transcriptional activity induced by UVB irradiation, showing that DHPV suppressed UVB-induced AP-1 transactivation in HDF (Fig. 5D). DHPV inhibits Capthesin G expression similar to that of CP (Fig. 5E). The concentrations of DHPV used in this experiment were not toxic to proliferation of human dermal fibroblast in the presence of UVB irradiation (Fig. 5F). These results indicated that CP metabolite DHPV may act as a driver to inhibit UVB-induced wrinkle formation by suppressing MMP-1 protein expression and gene transcription by inhibiting AP-1 activity in HDF.

Discussion

UVB is the major etiological factor of skin photoaging and carcinogenesis. In our previous studies, we measured the minimal UVB dose on the dorsal skin of the mice as the minimal edema dose (MEdD), setting MEdD as 100 mJ/cm^2. According to study of Bernerd *et al.*, daily dose of UV on earth is 100~200 J/cm^2 and average ratio of UVA/UVB is 27.3 (Marionnet *et al.*, 2015). Based on the calculation of physiological UVB dose, 200 mJ/cm^2 of UVB was used in this study: Average UVB dose of about 2 h activity in outside [37.75 J/cm^2 (UV dose of New York)/28.3(UVB/UV)/14 (day time) = 95 mJ/h cm^2].

CP-supplemented diets have been suggested to elicit many beneficial effects, particularly for skin health (Park *et al.*, 2014). In the present study, we investigated the anti-wrinkle effects of CP *in vivo*. Oral administration of CP reduced UVB-induced wrinkle formation and prevented UVB-induced collagen degradation in hairless mice. We also used a human equivalent skin model and primary human skin fibroblasts, and found that CP inhibits UVB-induced MMP-1 expression in both models. In addition, our clinical study shows that CP (4g/day for 24 weeks) significantly reduces wrinkle formation without side effects (data not shown). To investigate the anti-wrinkling mechanisms of CP, we performed an RNA SEQ array. 788 genes were found to be up- or down-regulated by CP treatment in UVB-irradiated skin tissues. Such significant changes in transcriptome may imply the existence of signature molecules to regulate UV-induced skin aging. Of particular note, cathepsin G was significantly inhibited whereas serpin b6c was upregulated in the presence of CP. Cathepsin G is known to induce fibronectin fragmentation (Son *et al.*, 2009). It has previously been reported that serpin b6 is a potent inhibitor of cathepsin G (Scott *et al.*, 1999). Although the detailed molecular relationship between skin wrinkling and cathepsin G activity has not been clearly elucidated, cathepsin G activity has in the past been linked to skin wrinkling (Son *et al.*, 2009), and is known to regulate MMP-1 mRNA expression (Son *et al.*, 2012). Our *in vivo* study shows that CP-supplementation inhibits UVB-induced skin wrinkling concurrent with the inhibition of cathepsin G and upregulation of serpin b6c. Cathepsin G expression was similarly inhibited by CP treatment in HDFs.

Intriguingly, we found that the CP-mediated skin response GRN included critical regulators of photoaging in skin such as NFE2L2 (Kawachi *et al.*, 2008; Tian *et al.*, 2011), peroxisome proliferator-activated receptor (PPAR) γ and TP53 (El-Domyati *et al.*, 2013; Lee *et al.*, 2012) (Fig. 3C). NFE2L2 is known as NF-E2-related factor2 (Nrf2) and a transcription activator that binds to antioxidant response (ARE) elements and Maf recognition elements in the promoter regions of target genes. Nrf2 is also important for the coordinated responses to oxidative stress (Itoh *et al.*, 2010; Sykiotis and Bohmann, 2010). UVA strongly induces Nrf2 expression in human skin fibroblasts but is weakly induced in skin keratinocytes. Knockdown of Nrf2 has been shown to markedly increase cell damage by UVA irradiation in skin keratinocytes, suggesting that Nrf2 may protect human skin keratinocytes from UVA radiation-induced damage (Tian *et al.*, 2011). Furthermore, UVB-induced sunburn reactions and oxidative DNA damage have been observed to be more prominent in *nrf2*$^{-/-}$ mice (Kawachi *et al.*, 2008). The photoprotective effect of Nrf2 is closely related to the inhibition of ECM degradation and inflammation (Saw *et al.*, 2014). Enhanced Nrf2 activity in keratinocytes has also been associated with epidermal barrier function and antioxidant defense (Schafer *et al.*, 2012). PPARs are a family of nuclear hormone receptors and play key roles in lipid metabolism and glucose homeostasis (Kota *et al.*, 2005; Kuenzli and Saurat, 2003; Lalloyer *et al.*, 2011; Varga *et al.*, 2011). Evidence suggests that PPARα/γ regulated gene responses have an effect on age-related inflammatory and photoaging mediators such as cytokines, MMPs, and AP-1, in NF-κB signaling (Chung *et al.*, 2008; Kim *et al.*, 2012; Michalik and Wahli, 2007). In addition, the tumor suppressor gene p53 plays an important role in protecting cells against DNA damage from sources of extrinsic stress (Nelson and Kastan, 1994). An earlier study has examined the significant impact of UVB on p53 (van Kranen *et al.*, 1997). Moreover, p53 is known to be activated by DNA damage, oxidative stress and inflammation (Ak and Levine, 2010; Han *et al.*, 2008; Nelson and Kastan, 1994; Reuter *et al.*, 2010), and has recently been identified as a UV target gene that associates with ^{V600E}BRAF to induce melanoma formation (Viros *et al.*, 2014). These genes could be novel candidates responsible for the CP-mediated UVB-protective effects observed. We also constructed a GRN composed of possible candidate TFs regulating cathepsin G and serpin b6c based on the unfiltered TF-target relationships in the ENCODE data. This GRN analysis suggested that the expression of these genes may be regulated by other transcription factors such as SPI1 and MAFK.

When human beings take in CP orally, it is then metabolized in the body. Namely, CP is changed into its metabolite and interacts with skin cells in form of metabolite. Various metabolites occur at digestion and absorption by CP consumption. According to the previous study (Urpi-Sarda *et al*., 2009), DHPV is mainly produced in plasma and appears the biggest variation after regular consumption of CP compared with before consumption of CP. Epicatechin and procyanidins which are major constituent in CP are metabolized into DHPV (Urpi-Sarda *et al*., 2009). We, then, hypothesized that the anti-wrinkle effect of CP may be derived from DHPV. As a result, DHPV suppressed UVB-induced MMP-1 protein expression and gene transcription by inhibiting AP-1 activity as the same as the effect of CP on those in HDF. DHPV, therefore, was considered to be active compound based on these results. Further studies should validate the various metabolites of CP of their effects on skin structure and developments.

Taken together, our studies indicate that CP supplementation contributes to a reduction in wrinkle formation and collagen degradation. Transcriptomic changes in response to UVB-irradiation in CP-supplemented mice provide evidence for an anti-photoaging effect of CP extract. Oral treatment of CP significantly down-regulates cathepsin G while up-regulating serpin b6c, which itself is known to inactivate cathepsin G. Therefore, CP supplementation may prevent breakdown of the dermal matrix. For clinical application, we examined the effects of CP and its major metabolites DHPV on photoaging in HDF. These results underline the potential for CP extracts to be further developed as anti-photoaging agents.

Materials and Methods

Preparation of CP

CP was provided by Barry Callebaut (Lebbeke-Wieze, Belgium). Cacao beans were roasted and ground to make cacao liquor, which was separated with cacao butter, to produce cacao cakes. CP was produced by grinding the cacao cakes. The flavanol content in the resultant CP was 71.5 mg/g, which was determined independently by the Korea Health Supplement Institute (Gyeonggi-do, Korea). CP was dissolved in 0.5% sodium carboxymethylcellulose for animal treatment and in 50% ethanol for cell treatment.

Animals and treatments

Six-week-old female albino hairless mice (Skh-1) were obtained from Bio Genomics, Inc. (Seoul, Korea). All experimental protocols were approved by the Institutional Animal Care and Use Committee (Case Number: 14-0008-S1A0) of the Biomedical Research Institute at Seoul National University Hospital. Groups of 8-10 mice were allocated to receive one of six treatment types. CP or a positive control were administered to the mice according to the following treatments groups: CP Low (39.1 mg/kg of CP), CP High (156.3 mg/kg of CP), and pycnogenol (positive control, 625 mg/kg of pycnogenol). CP and vehicle (0.5% sodium carboxymethylcellulose) were orally administered for 8 weeks, and body weight and food intake were monitored on a weekly basis. A photoaging experiment was also performed, as described previously (Kim *et al.*, 2005). A UVB irradiation device containing TL20W/12RS UV lamps (Philips, Eindhoven, Netherlands) with an emission spectrum between 275 and 380 nm (peak, 310–315 nm) served as the UV source. A Kodacel filter (TA401/407; Eastman Kodak, Rochester, NY) was mounted 2 cm in front of the UV lamp to remove wavelengths of less than 290 nm (UVC) (Seo *et al.*, 2001). Initially, we measured the minimal UVB dose on the dorsal skin of the mice as the MEdD comparable with a minimal erythema dose in human skin. In contrast to human skin, mouse skin showed peak responses to UVB primarily as edema, manifesting as an increased thickness of dorsal skin at 48 hours post-UVB irradiation (Benavides *et al.*, 2009; Learn *et al.*, 1995). The irradiation doses were increased weekly in increments of 0.5 MEdD (1 MEdD = 100 mJ/cm^2) up to 2 MEdD and then maintained at 2 MEdD thereafter. UVB irradiation was stopped after 8 weeks (Fig. 1A) (Jin *et al.*, 2010; Kim *et al.*, 2013; Park *et al.*, 2014; Yoon *et al.*, 2014).

RNA sequencing analysis

For the transcriptome analysis, frozen skin tissue was pulverized in liquid nitrogen, and total RNA was isolated using an RNeasy Plus Mini Kit (Qiagen, Valencia, CA) according to the manufacturer's instructions. The integrity of the RNA was assessed by 1% agarose gel electrophoresis and visualization of the 18S and 28S RNA species after ethidium bromide staining. RNA sequencing was performed by TheragenEtex Inc. DEGs in CL- and CH-fed mice skin irradiated with UVB were identified by comparing with the normal diet-fed mice irradiated with UVB using both 2-fold criteria and $P<0.05$ value cut-offs obtained from student's t-test. We then amalgamated the two DEG groups (in CL- and CH-fed mice) into CP-mediated DEGs.

GRN analysis

We constructed the CP-mediated skin response GRN by retrieving a reliable human GRN from the study by Gertein *et al*. (Gerstein *et al.*, 2012) and SignaLink Version 2 (Fazekas *et al.*, 2013) as follows: The significant TFs for the human homologs of the CP-mediated DEGs for were obtained by performing hypergeometric tests between the DEGs and a target gene group for a TF using both the $P< 0.05$ criteria and the size of the intersection between the DEG group and a target gene group > 1 criteria. We then amalgamated the significant TFs and their target genes into the CP-mediated skin response GRN. The CP-mediated skin response GRN was composed of two isolated connected components (Fig. 3C and 3D).

Cell culture and treatments

Primary human dermal fibroblasts (HDFs) were isolated from the outgrowth of foreskin obtained healthy 12 year-old volunteers with the approval of the Institutional Review Board of Seoul National University Hospital (Approval No. H-1101-116-353) and Seoul National University (No. E1408/001-002). HDFs were cultured in DMEM with 10% (v/v) FBS and 1% (v/v) penicillin/streptomycin at 37°C and 5% CO_2. Serum-starved monolayer cultures of HDF were exposed to UVB irradiation and treated with CP dissolved in 50% ethanol. HDFs were exposed to UVB at a dose of 0.02 J/cm^2 using a UVB source (Bio-Link crosslinker, VilberLourmat, Cedex 1, France) with a spectral peak set at 312 nm.

Preparation of human skin equivalent model

Neoderm®-ED, a human skin equivalent model, was purchased from TEGO Science (Seoul, Korea). Briefly, HDFs were cultured onto a collagen matrix for 1 day, before keratinocytes were seeded on top of the matrix and co-cultured for 4 days. Next, the keratinocytes and HDF block were raised for exposure to the air. CP was treated for 1 h after 12 days of air exposure. The human skin equivalent layer was then irradiated with 0.05 J/cm^2 UVB twice per day for 8 days. Media was changed every 2 days, and the layer was incubated at 37°C with 5% CO_2.

Assessment of wrinkle formation

To determine the severity of wrinkling, each hairless mouse was anesthetized and their UVB-exposed dorsal skin (wrinkle formation area) was photographed. The severity of wrinkling was measured by four trained graders using the Bissett's visual wrinkle scale (Bissett *et al.*, 1987). A skin wrinkle replica was made with silicone rubber (Silflo Dental Impression Materials, Potters Bar, UK) from the backs of untreated mice. This was photographed using a coupling charge system video camera. Wrinkle severity was assessed using a photographic scale (0, none; 1, minimal; 2, mild; 3, moderate; 4, severe; and 5, very severe) and analyzed by Skin-Visiometer SV 600 software (CK Electronic GmbH, Köln, Germany). The visiometer consists of a computerized instrument that creates a skin microrelief map from the replica using a light transmission method.

General laboratory experiments such as RT-PCR, Western Blotting Masson's trichrome staining, immunohistochemistry and luciferase reporter gene assay are described in supplement materials and methods

Statistical analysis

Statistical analyses were performed using one-way ANOVA followed by Duncan's statistical range test. *P* values of less than 0.05 were considered statistically significant.

Conflict of Interest

The authors state no conflict of interest

Acknowledgement

This work was supported by the R&D program of MOTIE/KIAT (Establishment of Infra Structure for Anti-aging Industry Support, No.N0000697) in Republic of Korea. We thank Jieun H. Kim for proofreading the manuscript and Dr. Akira Oshima for helping histological analysis.

References

Ak P, Levine AJ. p53 and NF-kappaB: different strategies for responding to stress lead to a functional antagonism. FASEB J 2010;24:3643-52.

Benavides F, Oberyszyn TM, VanBuskirk AM, Reeve VE, Kusewitt DF. The hairless mouse in skin research. J Dermatol Sci 2009;53:10-8.

Bissett DL, Hannon DP, Orr TV. An animal model of solar-aged skin: histological, physical, and visible changes in UV-irradiated hairless mouse skin. Photochem Photobiol 1987;46:367-78.

Bradley EJ, Griffiths CE, Sherratt MJ, Bell M, Watson RE. Over-the-counter anti-ageing topical agents and their ability to protect and repair photoaged skin. Maturitas 2015;80:265-72.

Cho HS, Lee MH, Lee JW, No KO, Park SK, Lee HS, et al. Anti-wrinkling effects of the mixture of vitamin C, vitamin E, pycnogenol and evening primrose oil, and molecular mechanisms on hairless mouse skin caused by chronic ultraviolet B irradiation. Photodermatol Photoimmunol Photomed 2007;23:155-62.

Chung JH, Seo AY, Chung SW, Kim MK, Leeuwenburgh C, Yu BP, et al. Molecular mechanism of PPAR in the regulation of age-related inflammation. Ageing Res Rev 2008;7:126-36.

Consortium EP. An integrated encyclopedia of DNA elements in the human genome. Nature 2012;489:57-74.

El-Domyati M, El-Ammawi TS, Medhat W, Moawad O, Mahoney MG, Uitto J. Expression of p53 protein after nonablative rejuvenation: the other side of the coin. Dermatol Surg 2013;39:934-43.

Fazekas D, Koltai M, Turei D, Modos D, Palfy M, Dul Z, et al. SignaLink 2 - a signaling pathway resource with multi-layered regulatory networks. BMC Syst Biol 2013;7:7.

Fisher GJ, Wang ZQ, Datta SC, Varani J, Kang S, Voorhees JJ. Pathophysiology of premature skin aging induced by ultraviolet light. N Engl J Med 1997;337:1419-28.

Gerstein MB, Kundaje A, Hariharan M, Landt SG, Yan KK, Cheng C, et al. Architecture of the human regulatory network derived from ENCODE data. Nature 2012;489:91-100.

Han ES, Muller FL, Perez VI, Qi W, Liang H, Xi L, et al. The in vivo gene expression signature of oxidative stress. Physiol Genomics 2008;34:112-26.

Heinrich U, Neukam K, Tronnier H, Sies H, Stahl W. Long-term ingestion of high flavanol cocoa provides photoprotection against UV-induced erythema and improves skin condition in women. J Nutr 2006;136:1565-9.

Ichihashi M, Ando H, Yoshida M, Niki Y, Matsui M. Photoaging of the skin. Anti-Aging Med 2009;6:46-59.

Itoh K, Mimura J, Yamamoto M. Discovery of the negative regulator of Nrf2, Keap1: a historical overview. Antioxid Redox Signal 2010;13:1665-78.

Jin XJ, Kim EJ, Oh IK, Kim YK, Park CH, Chung JH. Prevention of UV-induced skin damages by 11,14,17-eicosatrienoic acid in hairless mice in vivo. J Korean Med Sci 2010;25:930-7.

Kang NJ, Lee KW, Lee DE, Rogozin EA, Bode AM, Lee HJ, et al. Cocoa procyanidins suppress transformation by inhibiting mitogen-activated protein kinase kinase. J Biol Chem 2008;283:20664-73.

Katz DL, Doughty K, Ali A. Cocoa and chocolate in human health and disease. Antioxid Redox Signal 2011;15:2779-811.

Kawachi Y, Xu X, Taguchi S, Sakurai H, Nakamura Y, Ishii Y, et al. Attenuation of UVB-induced sunburn reaction and oxidative DNA damage with no alterations in UVB-induced skin carcinogenesis in Nrf2 gene-deficient mice. J Invest Dermatol 2008;128:1773-9.

Kim HH, Lee MJ, Lee SR, Kim KH, Cho KH, Eun HC, et al. Augmentation of UV-induced skin wrinkling by infrared irradiation in hairless mice. Mech Ageing Dev 2005;126:1170-7.

Kim JE, Son JE, Jung SK, Kang NJ, Lee CY, Lee KW, et al. Cocoa polyphenols suppress TNF-alpha-induced vascular endothelial growth factor expression by inhibiting phosphoinositide 3-kinase (PI3K) and mitogen-activated protein kinase kinase-1 (MEK1) activities in mouse epidermal cells. Br J Nutr 2010;104:957-64.

Kim JK, Mun S, Kim MS, Kim MB, Sa BK, Hwang JK. 5,7-Dimethoxyflavone, an activator of PPARalpha/gamma, inhibits UVB-induced MMP expression in human skin fibroblast cells. Exp Dermatol 2012;21:211-6.

Kim MK, Lee S, Kim EJ, Kong KH, Lee DH, Chung JH. Topical application of anacardic acid (6-nonadecyl salicylic acid) reduces UV-induced histone modification, MMP-13, MMP-9, COX-2 and TNF-alpha expressions in hairless mice skin. J Dermatol Sci 2013;70:64-7.

Kota BP, Huang TH, Roufogalis BD. An overview on biological mechanisms of PPARs. Pharmacol Res 2005;51:85-94.

Kuenzli S, Saurat JH. Effect of topical PPARbeta/delta and PPARgamma agonists on plaque psoriasis. A pilot study. Dermatology 2003;206:252-6.

Lalloyer F, Wouters K, Baron M, Caron S, Vallez E, Vanhoutte J, et al. Peroxisome proliferator-activated receptor-alpha gene level differently affects lipid metabolism and inflammation in apolipoprotein E2 knock-in mice. Arterioscler Thromb Vasc Biol 2011;31:1573-9.

Learn DB, Beasley DG, Giddens LD, Beard J, Stanfield JW, Roberts LK. Minimum doses of ultraviolet radiation required to induce murine skin edema and immunosuppression are different and depend on the ultraviolet emission spectrum of the source. Photochem Photobiol 1995;62:1066-75.

Lee KW, Kim YJ, Lee HJ, Lee CY. Cocoa has more phenolic phytochemicals and a higher antioxidant capacity than teas and red wine. J Agric Food Chem 2003;51:7292-5.

Lee KW, Kundu JK, Kim SO, Chun KS, Lee HJ, Surh YJ. Cocoa polyphenols inhibit phorbol ester-induced superoxide anion formation in cultured HL-60 cells and expression of cyclooxygenase-2 and activation of NF-kappaB and MAPKs in mouse skin in vivo. J Nutr 2006;136:1150-5.

Lee YK, Cha HJ, Hong M, Yoon Y, Lee H, An S. Role of NF-kappaB-p53 crosstalk in ultraviolet A-induced cell death and G1 arrest in human dermal fibroblasts. Arch Dermatol Res 2012;304:73-9.

Marini A, Grether-Beck S, Jaenicke T, Weber M, Burki C, Formann P, et al. Pycnogenol(R) effects on skin elasticity and hydration coincide with increased gene expressions of collagen type I and hyaluronic acid synthase in women. Skin Pharmacol Physiol 2012;25:86-92.

Marionnet C, Tricaud C, Bernerd F. Exposure to non-extreme solar UV daylight: spectral characterization, effects on skin and photoprotection. Int J Mol Sci 2015;16:68-90.

Michalik L, Wahli W. Peroxisome proliferator-activated receptors (PPARs) in skin health, repair and disease. Biochim Biophys Acta 2007;1771:991-8.

Nelson WG, Kastan MB. DNA strand breaks: the DNA template alterations that trigger p53-dependent DNA damage response pathways. Mol Cell Biol 1994;14:1815-23.

Neukam K, Stahl W, Tronnier H, Sies H, Heinrich U. Consumption of flavanol-rich cocoa acutely increases microcirculation in human skin. Eur J Nutr 2007;46:53-6.

Park HS, Jin SP, Lee Y, Oh IG, Lee S, Kim JH, et al. Toll-like receptor 2 mediates a cutaneous reaction induced by repetitive ultraviolet B irradiation in C57/BL6 mice in vivo. Exp Dermatol 2014;23:591-5.

Reuter S, Gupta SC, Chaturvedi MM, Aggarwal BB. Oxidative stress, inflammation, and cancer: how are they linked? Free Radic Biol Med 2010;49:1603-16.

Saw CL, Yang AY, Huang MT, Liu Y, Lee JH, Khor TO, et al. Nrf2 null enhances UVB-induced skin inflammation and extracellular matrix damages. Cell Biosci 2014;4:39.

Scapagnini G, Davinelli S, Di Renzo L, De Lorenzo A, Olarte HH, Micali G, et al. Cocoa bioactive compounds: significance and potential for the maintenance of skin health. Nutrients 2014;6:3202-13.

Schafer M, Farwanah H, Willrodt AH, Huebner AJ, Sandhoff K, Roop D, et al. Nrf2 links epidermal barrier function with antioxidant defense. EMBO Mol Med 2012;4:364-79.

Scott FL, Hirst CE, Sun J, Bird CH, Bottomley SP, Bird PI. The intracellular serpin proteinase inhibitor 6 is expressed in monocytes and granulocytes and is a potent inhibitor of the azurophilic granule protease, cathepsin G. Blood 1999;93:2089-97.

Scott FL, Sun J, Whisstock JC, Kato K, Bird PI. SerpinB6 is an inhibitor of kallikrein-8 in keratinocytes. J Biochem 2007;142:435-42.

Seo JY, Lee SH, Youn CS, Choi HR, Rhie GE, Cho KH, et al. Ultraviolet radiation increases tropoelastin mRNA expression in the epidermis of human skin in vivo. J Invest Dermatol 2001;116:915-9.

Son ED, Kim H, Choi H, Lee SH, Lee JY, Kim S, et al. Cathepsin G increases MMP expression in normal human fibroblasts through fibronectin fragmentation, and induces the conversion of proMMP-1 to active MMP-1. J Dermatol Sci 2009;53:150-2.

Son ED, Shim JH, Choi H, Kim H, Lim KM, Chung JH, et al. Cathepsin G inhibitor prevents ultraviolet B-induced photoaging in hairless mice via inhibition of fibronectin fragmentation. Dermatology 2012;224:352-60.

Subhashini R, Mahadeva Rao US, Sumathi P, G. G. A comparative phytochemical analysis of cocoa and green tea. Indian J Sci and Tech 2010;3:188-92.

Sykiotis GP, Bohmann D. Stress-activated cap'n'collar transcription factors in aging and human disease. Sci Signal 2010;3:re3.

Tian FF, Zhang FF, Lai XD, Wang LJ, Yang L, Wang X, et al. Nrf2-mediated protection against UVA radiation in human skin keratinocytes. Biosci Trends 2011;5:23-9.

Urpi-Sarda M, Monagas M, Khan N, Llorach R, Lamuela-Raventos RM, Jauregui O, et al. Targeted metabolic profiling of phenolics in urine and plasma after regular consumption of cocoa by liquid chromatography-tandem mass spectrometry. J Chromatogr A 2009;1216:7258-67.

van Kranen HJ, de Laat A, van de Ven J, Wester PW, de Vries A, Berg RJ, et al. Low incidence of p53 mutations in UVA (365-nm)-induced skin tumors in hairless mice. Cancer Res 1997;57:1238-40.

Varga T, Czimmerer Z, Nagy L. PPARs are a unique set of fatty acid regulated transcription factors controlling both lipid metabolism and inflammation. Biochim Biophys Acta 2011;1812:1007-22.

Viros A, Sanchez-Laorden B, Pedersen M, Furney SJ, Rae J, Hogan K, et al. Ultraviolet radiation accelerates BRAF-driven melanomagenesis by targeting TP53. Nature 2014;511:478-82.

Xu Y, Fisher GJ. Ultraviolet (UV) light irradiation induced signal transduction in skin photoaging. Journal of Dermatological Science Supplement 2005;1:S1-S8.

Yoon HS, Shin CY, Kim YK, Lee SR, Chung JH. Endogenous estrogen exacerbates UV-induced inflammation and photoaging in mice. J Invest Dermatol 2014;134:2290-3.

Zheng Y, Lai W, Wan M, Maibach HI. Expression of cathepsins in human skin photoaging. Skin Pharmacol Physiol 2011;24:10-21.

Figure Legends

Figure 1. Effect of cacao powder (CP) on UVB-induced wrinkle formation. (a) A schematic diagram of the animal experiment. (b) Back skins of hairless mice (8-10 mice per each group) were exposed to UVB for 8 weeks as scheduled in (A). Bottom figures are replica from back of mice as developed in materials and methods (c) Skin impressions were analyzed by Skin-Visiometer software after 8 weeks of treatment. (d) The severity of skin wrinkling was visually graded as described in the Materials and Methods after 8 weeks of treatment. Data represent the means ± SEM (n = 8-10). Means with letters (a-c) within a graph are significantly different from each other at $p<0.05$. (e) Masson's trichrome staining for collagen fibers. Collagen fibers appear blue. Scale bar = 100 µm. (A) The vehicle was 0.5% sodium carboxymethylcellulose. (B) UVB, (C) UVB+ CL (low concentration of CP), (D) UVB+CH (high concentration of CP) and (E) UVB+Pyc (Pycnogenol). (f) Expression profile of differentially expressed genes (DEGs) mediated by CP in mouse skin tissue. Heat map of DEGs mediated by low or high CP concentration. Expression of genes represent log2 ratio of indicated group. (g) Heat map of DEGs up-regulated by UVB and down-regulated by high concentrations of CP. (h) Heat map of DEGs down-regulated by UVB and up-regulated by high concentrations of CP. Heat maps (g and h) are drawn based on Log2 FPKM of each group. Blue color indicates low expression of genes in each group while red color represents high level of gene expression.

Figure 2. Expression of genes involved in dermal matrix formation, following GO terms. Expression profiles of DEGs were classified by GO terms as follows (a) Extracellular Matrix Disassembly, (b) Cell Adhesion, (c) Lipid Metabolic Process, and (d) Proteinaceous Extracellular Matrix. Bar-graph shows the relative log2 mRNA ratio of the indicated targets from RNA sequence data of each group with statically significance (P<0.05).

Figure 3. CP regulates the expression of extracellular matrix (ECM) genes. (a) CP supplementation significantly inhibits expression of cathepsin G in UVB-irradiated skin tissue. (b) The expression of Serpin B6c is markedly enhanced by CP supplementation. The graph is representative of the RNA sequence analyses from five mice. Bars followed by the same letter do not differ significantly ($P<0.05$). (c) The largest connected component of CP-mediated skin response Gene Regulatory Network (GRN). (d) The second largest connected component of the GRN in response to UVB and CP administration. GRNs were constructed as described in materials and methods. (e) Candidates of transcription factors (TFs) that regulate the specific target genes such as Cathepsin G, Serpin B6c, Collagen 25A1 (COL25A1), and Fibronectin 1 (FN1). Hexagon nodes with green borders denote TFs. Red and blue nodes denote up-regulated and down-regulated genes by high concentrations of CP, respectively.

Figure 4. CP inhibits UVB induced MMP-1 expression in human dermal fibroblast (HDF) and human skin equivalent (HSE). (a) CP inhibits the expression of UVB-induced MMP-1. MMP-2 is used as a loading control. (b) MMP-1 mRNA levels for the CP group are analyzed by real-time quantitative PCR (RT-qPCR). Data (n = 3) represent the means ± SD. (c) Regulation of AP-1 transcriptional activity by CP. A luciferase reporter gene assay was performed in HDF as described in the materials and methods. (d) Cell viability after CP treatment. Cell viability is measured using the CellTiter 96® AQueous One Solution Cell Proliferation Assay. (A-D) HDF cells are pretreated with CP at the indicated concentrations for 1 h, and then further treated with 0.02 J/cm^2 UVB for 48 h at 37 °C. Data (n = 4) represent the means ± SD. Means with letters (a-e) within a graph are significantly different from each other at $p<0.05$. (e) Cathepsin G expression is inhibited by CP. Treatment of CP and UVB is the same as described in (a-d). (f) CP inhibits UVB-induced MMP-1 protein expression in HSE. HSE was developed as described in Schematic diagram of HSE system (Supplement figure 2). HSE serial sections from the human skin equivalent were mounted onto silane-coated slides and subjected to immunohistochemical staining using anti-MMP-1 antibody as described in the Materials and Methods. Scale bar = 50 µm,

Figure 5. A major metabolite, 5-(3´,4´-dihydroxyphenyl)-ɣ-valerolactone (DHPV) inhibits UVB-induced MMP-1 protein expression, gene transcription and AP-1 transactivation in HDF. (a) Chemical structure of DHPV. (b) Expression of MMP-1 was inhibited by DHVP under UVB-IR in HDF. MMP-2 was used as a loading control. (c) Suppression of MMP-1 mRNA expression by DHVP was analyzed by RT-qPCR. Triplicate samples were used and experiments were repeated three times; the mean ± SD. (d) The effect of DHVP on AP-1 transcriptional activity in HDF. AP-1 transactivation ability was measured by a luciferase reporter gene assay. Data (n = 3) represent the mean ± SD. (c-d) Means with letter (a-c) within a graph are significantly different from each other at $p<0.05$. (e) Inhibition of UVB-induced Cathepsin G expression by DHPV. (f) DHPV did not affect cell viability. Data (n = 8) represent the mean ± SD. Means with letter (a) within a graph are no significantly different from each other at $p < 0.05$. (b-f) Conditions of treatment of DHPV and UVB in HDF are the same as described in Fig. 4.

Figure 1

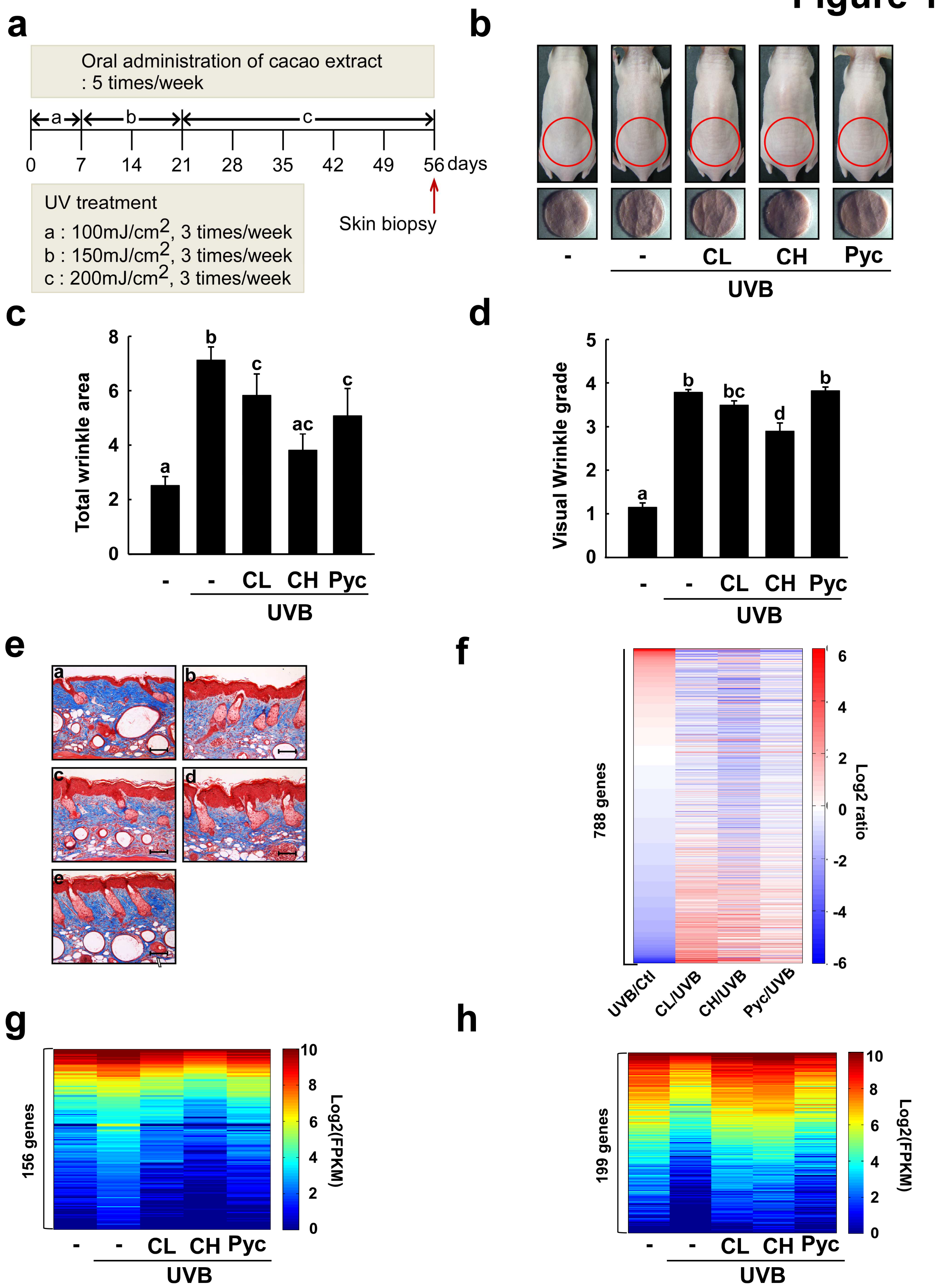
a
Oral administration of cacao extract
: 5 times/week
a
b
c
0
7
14
21
28
35
42
49
56 days
Skin biopsy
UV treatment
a : 100mJ/cm2, 3 times/week
b : 150mJ/cm2, 3 times/week
c : 200mJ/cm2, 3 times/week
b
- - CL CH Pyc
UVB
c
Total wrinkle area
- - CL CH Pyc
UVB
d
Visual Wrinkle grade
- - CL CH Pyc
UVB
e
f
788 genes
Log2 ratio
UVB/Ctl
CL/UVB
CH/UVB
Pyc/UVB
g
156 genes
Log2(FPKM)
- - CL CH Pyc
UVB
h
199 genes
Log2(FPKM)
- - CL CH Pyc
UVB

Figure 2

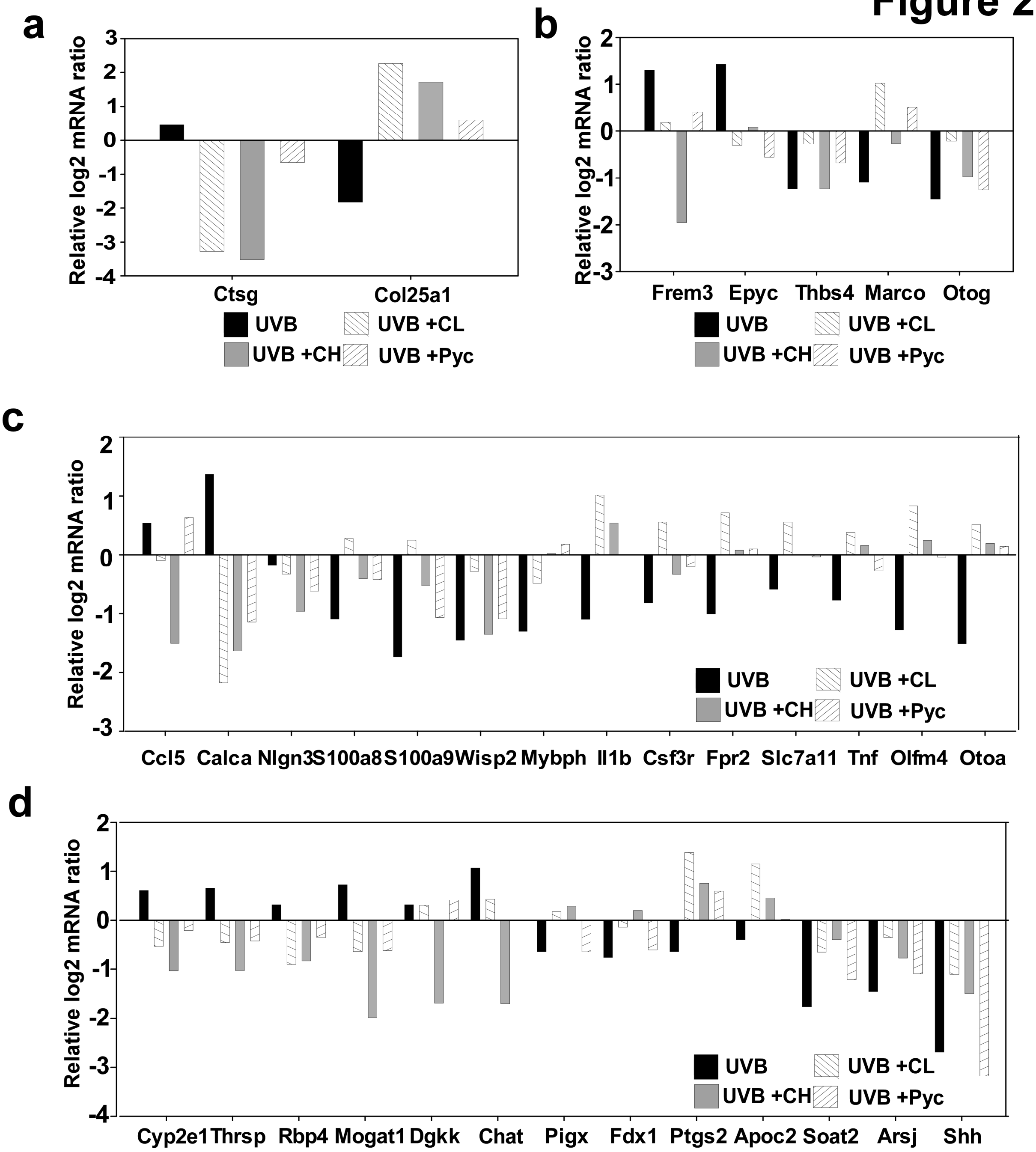
a
Relative log2 mRNA ratio
3
2
1
0
-1
-2
-3
-4
Ctsg
Col25a1
UVB
UVB +CL
UVB +CH
UVB +Pyc
b
Relative log2 mRNA ratio
2
1
0
-1
-2
-3
Frem3
Epyc
Thbs4
Marco
Otog
UVB
UVB +CL
UVB +CH
UVB +Pyc
c
Relative log2 mRNA ratio
2
1
0
-1
-2
-3
Ccl5
Calca
Nlgn3
S100a8
S100a9
Wisp2
Mybph
Il1b
Csf3r
Fpr2
Slc7a11
Tnf
Olfm4
Otoa
UVB
UVB +CL
UVB +CH
UVB +Pyc
d
Relative log2 mRNA ratio
2
1
0
-1
-2
-3
-4
Cyp2e1
Thrsp
Rbp4
Mogat1
Dgkk
Chat
Pigx
Fdx1
Ptgs2
Apoc2
Soat2
Arsj
Shh
UVB
UVB +CL
UVB +CH
UVB +Pyc

Figure 3

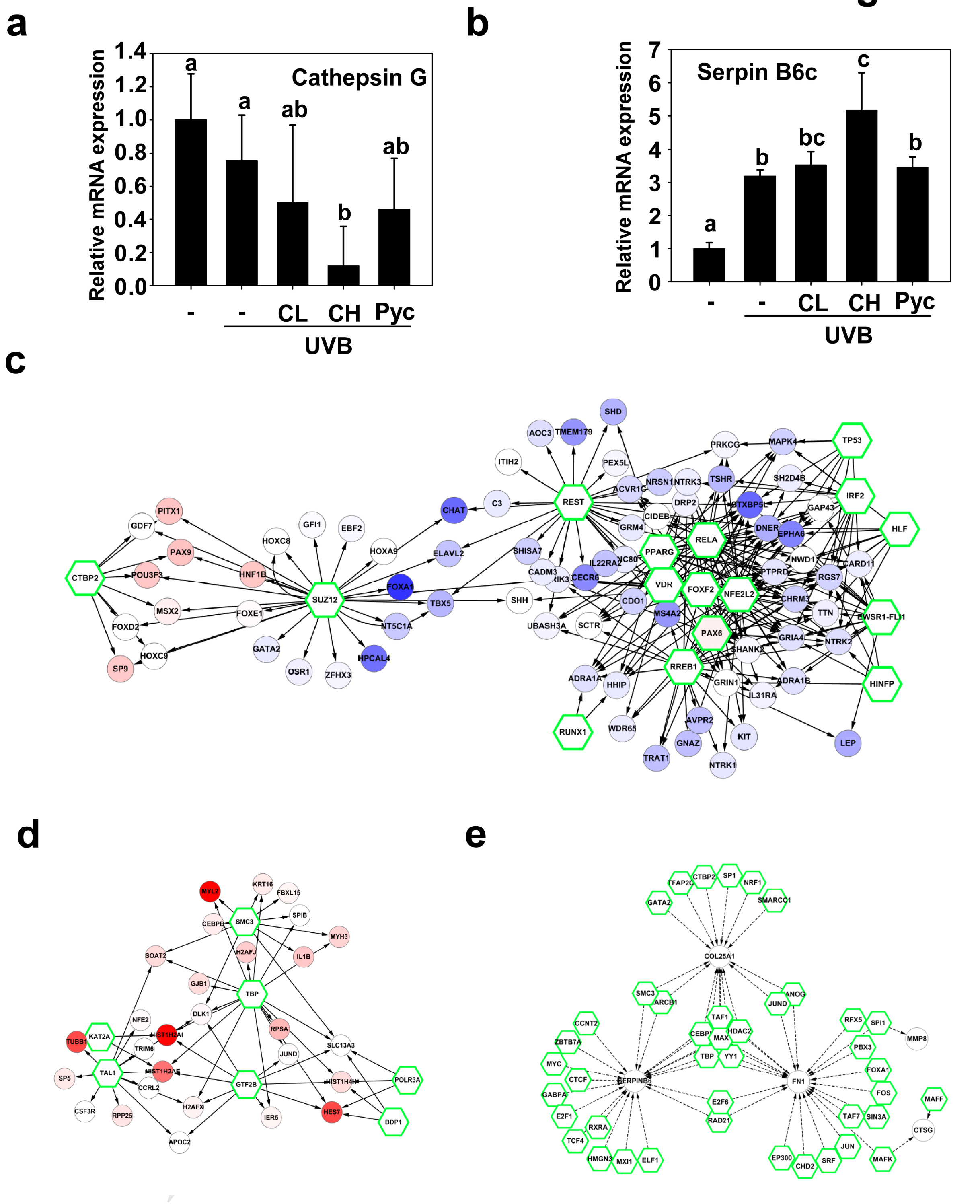

a
Cathepsin G
Relative mRNA expression
1.4
1.2
1.0
0.8
0.6
0.4
0.2
0.0
a
a
ab
b
ab
-
-
CL
CH
Pyc
UVB
b
Serpin B6c
Relative mRNA expression
7
6
5
4
3
2
1
0
a
b
bc
c
b
-
-
CL
CH
Pyc
UVB
c
d
e

Figure 4

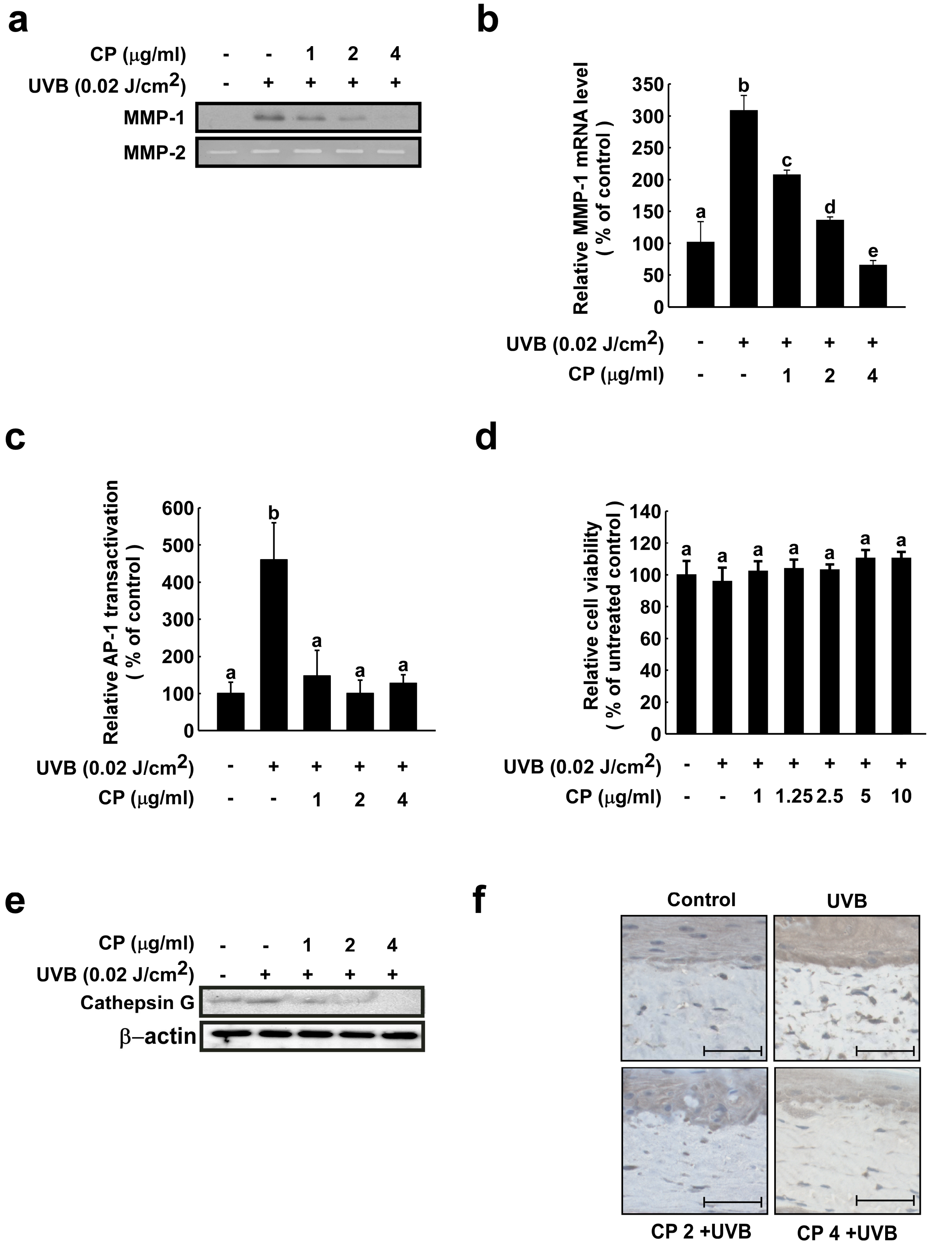
a
CP (μg/ml) - - 1 2 4
UVB (0.02 J/cm2) - + + + +
MMP-1
MMP-2
b
Relative MMP-1 mRNA level (% of control)
350
300
250
200
150
100
50
0
b
c
a
d
e
UVB (0.02 J/cm2) - + + + +
CP (μg/ml) - - 1 2 4
c
Relative AP-1 transactivation (% of control)
600
500
400
300
200
100
0
b
a
UVB (0.02 J/cm2) - + + + +
CP (μg/ml) - - 1 2 4
d
Relative cell viability (% of untreated control)
140
120
100
80
60
40
20
0
a
UVB (0.02 J/cm2) - + + + + + +
CP (μg/ml) - - 1 1.25 2.5 5 10
e
CP (μg/ml) - - 1 2 4
UVB (0.02 J/cm2) - + + + +
Cathepsin G
β–actin
f
Control
UVB
CP 2 +UVB
CP 4 +UVB

Figure 5

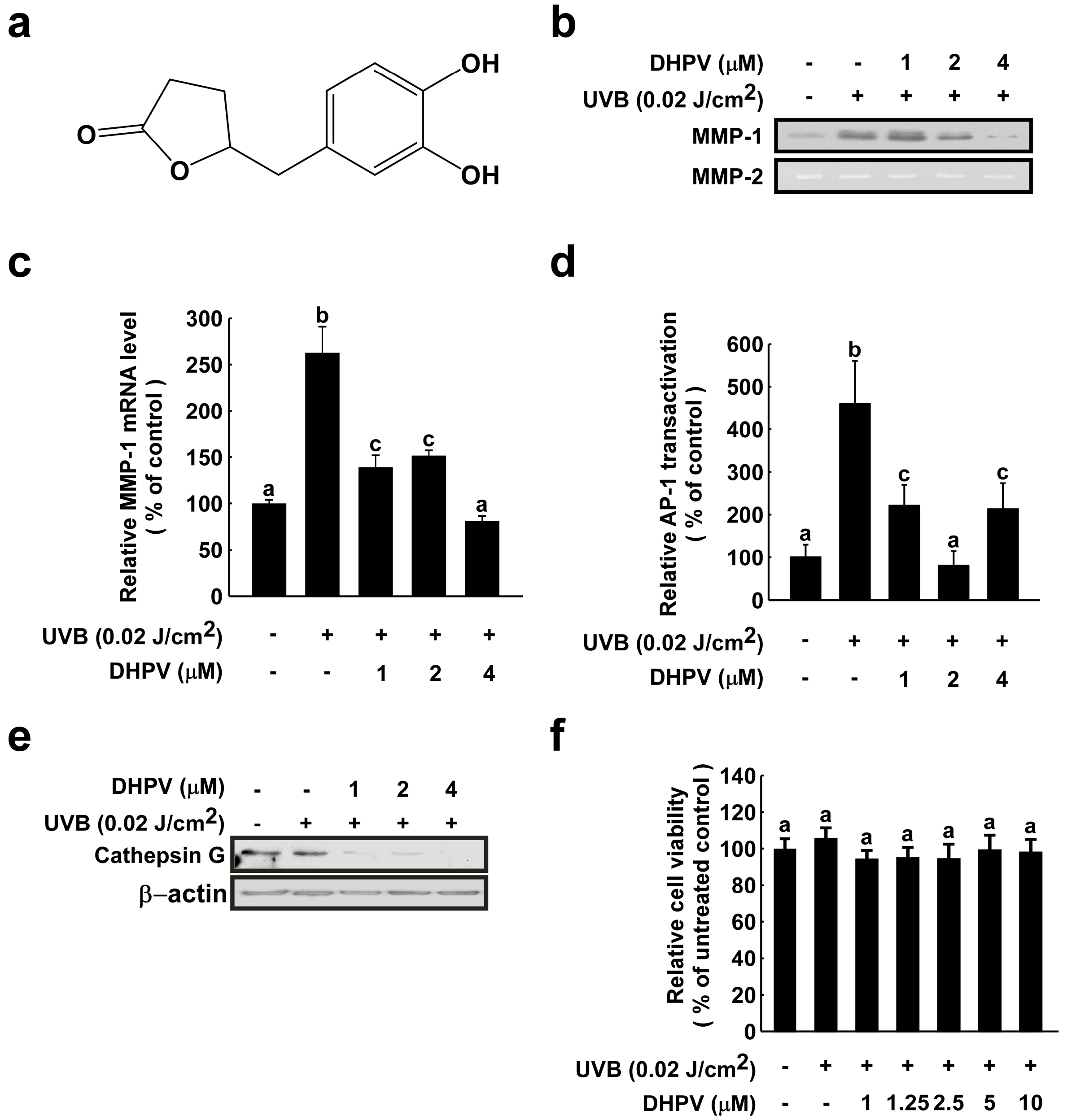
a
OH
O
O
OH
b
DHPV (μM) - - 1 2 4
UVB (0.02 J/cm2) - + + + +
MMP-1
MMP-2
c
Relative MMP-1 mRNA level (% of control)
300
250
200
150
100
50
0
a b c c a
UVB (0.02 J/cm2) - + + + +
DHPV (μM) - - 1 2 4
d
Relative AP-1 transactivation (% of control)
600
500
400
300
200
100
0
a b c a c
UVB (0.02 J/cm2) - + + + +
DHPV (μM) - - 1 2 4
e
DHPV (μM) - - 1 2 4
UVB (0.02 J/cm2) - + + + +
Cathepsin G
β–actin
f
Relative cell viability (% of untreated control)
140
120
100
80
60
40
20
0
a a a a a a a
UVB (0.02 J/cm2) - + + + + + +
DHPV (μM) - - 1 1.25 2.5 5 10